Available online at www.sciencedirect.com
SCIENCE DIRECT
Building and Environment 41 (2006) 851–863
BUILDING AND ENVIRONMENT
www.elsevier.com/locate/buildenv

Effects of inlet and exhaust locations and emitted gas density on indoor air contaminant concentrations

J.A. Khan[a,*], C.E. Feigley[b], E. Lee[b], M.R. Ahmed[a], S. Tamanna[a]

[a]Department of Mechanical Engineering, University of South Carolina, Columbia, SC 29208, USA
[b]Department of Environmental Health Sciences, University of South Carolina, Columbia, SC 29208, USA

Received 5 April 2004; received in revised form 7 October 2004; accepted 4 April 2005

Abstract

The steady-state distribution of contaminant concentrations in a workroom is a function of several factors, of which the types and relative position of air inlets and exhausts are some of the most important. Here several different inlet and exhaust locations and types (with or without diffuser) were investigated to determine the optimum inlet and exhaust positions. Room concentration patterns for a workroom were explored by computational fluid dynamics (CFD) simulations for various inlet locations, exhaust locations, contaminant gas densities, and dilution air flow rates. Average contaminant concentrations were calculated for the entire room, the breathing zone plane, and the near-source breathing zone (BZ).

The computational results were validated with experimental results. For wall jet inlets and for lighter than air, the exhausts located near the ceiling resulted in lower concentrations than the corresponding exhausts near the floor. Also, the exhausts located on the same wall as the inlet were relatively better than that of the opposite side wall. The relative density of the contaminant was found to have some effects on the concentration distribution at low flow rates, whereas this effect was negligible at higher flow rates (8 ACH or higher). Exhaust location was not important for ceiling inlets as the room was well mixed. Although ceiling inlet type had almost no effect on average concentration, near-source concentrations were markedly less for the ceiling jet inlet than for the ceiling diffuser inlet.

1. Introduction

Human exposure to indoor air pollutants is a function of contaminant distribution patterns in workrooms. The ability to understand contaminant transport and the resulting concentration pattern is important to occupational hygienists and other occupational health professionals. A clear understanding of the factors affecting the transport and distribution of airborne contaminants leads to improved design and ventilation of workrooms and helps minimize worker exposures. Several approaches have been undertaken to assess the concentration of contaminants, some of these methods involve on-site measurements and/or scale model experiments, both of which can be expensive. In addition to experimental determinations, predictive models have been used to ascertain the airborne contaminant concentrations in rooms. Models describing the relationship of contaminant emission rate (G), dilution air flow rate (Q), and the airborne contaminant concentration (C) in an enclosed space are important tools for estimating worker exposure. However, most of these models are based on simplistic assumptions regarding air flow and contaminant transport. In a c*ompletely mixed (CM) model,* the contaminant concentration in a room or portions of a room are assumed to be uniform. However, no workroom with localized sources and dilution air exchange has perfectly uniform concentration. Thus it is important to understand the impact of non-uniform concentration on errors in estimating exposure. With recognition that

*Corresponding author. Tel.: +1 803 777 1578; fax: +1 803 777 0106.
E-mail address: khan@engr.sc.edu (J.A. Khan).

0360-1323/$ - see front matter
doi:10.1016/j.buildenv.2005.04.002

concentration field in a room especially near the contaminant source, is not uniform, improvements were proposed by several researchers [1–5]. The next level of sophistication of the CM model is to utilize *multiple zones* within a space, each of which is assumed to be completely mixed. This was suggested by Hemeon [6], more recently discussed by Heinsohn [7], and used to illustrate the deficiencies of using mixing factors by Nicas [8]. Sherman [10] discussed and used tracer gas techniques—continuity equation, tracer decay, long term integral, and constant concentration—to measure ventilation in a single zone. Multi-zone models were further studied by Waters and Simons [11], Feigley et al. [12] and Nicas and Jayjock [13]. A further improvement on these models was achieved by the *Uniform Diffusivity (UD) Model.* This model assumes that the contaminant transport away from the source is due to turbulent diffusion, the intermingling and mixing of parcels of air (eddies), resulting in a net movement of contaminant from high to low concentration regions. A typical formulation of this model for isotropic diffusion from a point source on a flat surface was derived by analogy with heat transfer [9].

In this paper, a detailed computational fluid dynamics (CFD) analysis CFD analysis is performed to study the effects of relative locations of inlet and exhaust ventilation ports, flow rates of ventilation air, and effects of contaminant density. The rationale for performing this research is that the effects of none of the variables mentioned can be determined by the mathematical models. Therefore, the authors believe that to fully understand the physics of room air concentration distribution, there is a need for an alternative research tool. Exposure assessment using state-of-the-art CFD analysis presents one such alternative. Exposure assessment using CFD modeling has demonstrated good agreement with real life situations and shows great promise. For example, the CFD-simulated 3-dimensional distribution of contaminant concentration using the inlet velocities measured in traverses across the air inlet showed good qualitative and quantitative agreement with measured room concentrations [14].

To accurately predict the distribution of airborne contaminants it is imperative to consider as many factors as possible that affect the contaminant distribution. There are several factors that affect the overall intensity of concentration throughout the room. Some of them are: 1) Air inlet—geometry, number, location, and type (with or without diffuser); 2) Contaminant source—type (evaporating or pure gas emitting), flow rate, location in the room and properties such as temperature, density, and diffusivity; 3) Exhaust—type (exhaust fan or simply open), location, number and geometry; 4) Room—size, geometry and relative position in the building; 5) Dilution air—temperature, pressure, humidity, purity and make-up air flow rate (ACH air changing per hour); 6) Wall and ceiling—surface condition and temperature; 7) Room inside objects (furniture or equipment)—type, number, location and heat sourcing capacity; and 8) Workers—type of works, age group, number, movement.

As mentioned earlier, none of the analytical models account for combined effects of some of the very important factors like the air inlet—geometry, number, location and type (with or without diffuser), make-up air flow rate, location in the room and properties such as temperature, density and diffusivity, and exhaust-type (exhaust fan or simply open).

A series of experimental tests to completely investigate the effect of relative inlet and exhaust locations, the effect of contaminant density, and the effect of ACH on contaminant concentration would be very expensive and time consuming. Presently, the rapid development in CFD simulation technique both in finite-volume approaches and finite-element approaches makes it more and more available for research. Here CFD modeling was validated and then used to assess the contaminant concentration. Among some of the important factors investigated in this paper are the location of air inlet and exhaust, ACH, density of the contaminant, ceiling air inlet type. A parametric study of the effect of ACH on the contaminant distribution in the breathing zone (BZ) and in the entire room (RA) was performed to find the optimal relative locations of air inlet and exhaust. Relative density of the contaminant compared to air is another factor that may affect the contaminant distribution was also studied. The effect of a ceiling inlet with and without diffuser was also analyzed. Although CFD requires powerful computing resources and detailed boundary conditions, its results are the most comprehensive and dependable if the domain is modeled perfectly with accurate boundary conditions. This has been demonstrated by validating the numerical results with experimental findings.

2. CFD analysis

2.1. Modeling

A 7.8 m $(L) \times 5.4$ m (W) $\times 3.0$ m (H) room was chosen for CFD simulations with an air inlet opening of $0.9\,\text{m} \times 0.3\,\text{m}$ on the side walls or $0.6\,\text{m} \times 0.6\,\text{m}$ in the ceiling, and an exhaust opening of $0.6\,\text{m} \times 0.6\,\text{m}$. A source table of $0.9\,\text{m}$ $(L) \times 0.9\,\text{m}(W) \times 1.0\,\text{m}$ (H) was located on the floor in the middle of the room. Contaminant gas emanated from a $0.3\,\text{m} \times 0.3\,\text{m}$ opening at a low flow rate of $1.40\text{E}{-}5\,\text{m}^3/\text{s}$. No other flow obstructions were in the room and there was no worker either.

Hexahedral structured mesh with 37284 cells of 0.15 m cube was modeled in Gambit 2.0, (Fluent Inc, Lebanon, NH). Steady-state segregated solver of finite-difference based CFD FLUENT 6.0 was used to solve the system of governing equations—conservation of mass, conservation of momentum, and species transport equation. Isothermal cases were studied.

The governing equations consisting of the conservation of mass, momentum and species for steady-state conditions were solved iteratively.

The mass conservation equation

$$\nabla \cdot (\rho\vec{v}) = 0.$$

Momentum conservation equations

$$\nabla \cdot (\rho\vec{v}\vec{v}) = -\nabla p + \nabla \cdot (\bar{\bar{\tau}}) + \rho\vec{g},$$

where p is the static pressure, $\rho\vec{g}$ is the gravitational body force, $\bar{\bar{\tau}}$ is the stress tensor defined as

$$\bar{\bar{\tau}} = \mu\left[(\nabla\vec{v} + \nabla\vec{v}^T) - \tfrac{2}{3}\nabla.\vec{v}I\right],$$

where μ is the molecular viscosity, I is the unit tensor, and the second term on the right-hand side is the effect of volume dilation.

Species transport equations

$$\nabla \cdot (\rho\vec{v}Y_i) = -\nabla \cdot \bar{J}_i,$$

where Y_i is local mass fraction of each species i and $\bar{J}_i$ is the diffusion flux of species i, which arises due to concentration gradients. For turbulent flows it is defined as

$$\bar{J}_i = -\left(\rho D_{i,m} + \frac{\mu_t}{Sc_t}\right)\nabla Y_i,$$

where Sc_t is the turbulent Schmidt number, (with $\frac{\mu_t}{\rho D_t}$ a default setting of 0.7).

Standard $k-\varepsilon$ turbulence model was chosen to model turbulence due to its simplicity and applicability for the flow under consideration. For the species transport modeling, mass diffusivity of 2.29E−05 m^2/s was assumed for mixture of air and tracer gas (density equal to air density) and the mixture density was calculated by Volume-Mixing-Law. For the second set of modeling to analyze the effect of the relative density of the contaminant, air and iso-butylene mixture was used with their default properties given in FLUENT CFD.

$$\rho = \frac{1}{\sum_i \frac{Y_i}{\rho_i}},$$

where Y_i is the mass fraction and ρ_i is the density of species i.

Velocity inlet boundary conditions for both air inlet and contaminant source were considered uniform and the flow was normal to inlet section. Contaminant inlet was assumed to be a gas-phase contaminant source. The standard FLUENT wall function (no slip, smooth and no diffusive flux of the species) was used. For discretization, the body force weighted scheme for pressure, the SIMPLE scheme for pressure-velocity coupling, and the first-order upwind scheme for

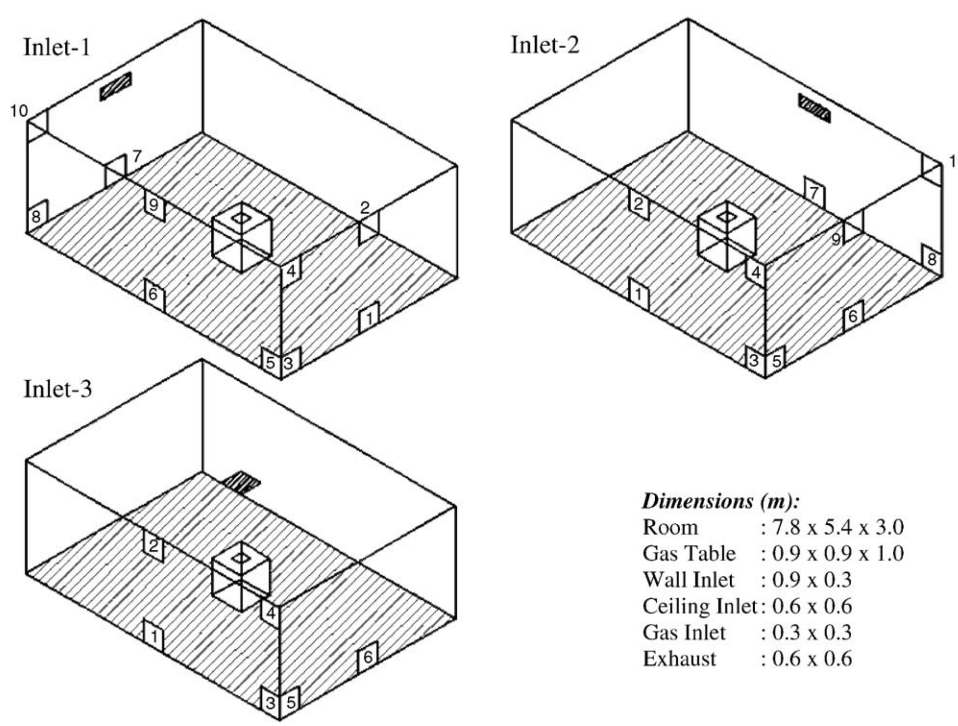

Fig. 1. Shows the room geometry with relative inlet and exhaust locations.

momentum, turbulence and species were chosen. Under-relaxation factors were manipulated to get quick convergence and solution was assumed to converge when the residuals for all scalars were less than or equal to 1.0E−06.

In FLUENT, scaled residual for segregated solver is defined as

$$R^{\phi} = \frac{\sum_{\text{cells } P} \left| \sum_{\text{nb}} a_{\text{nb}} \phi_{\text{nb}} + b - a_p \phi P \right|}{\sum_{\text{cells } P} |a_p \phi P|},$$

where ϕ is any variable of interest for which residual is to be calculated, P is any cell, a_P is the center coefficient, $a_{\text{nb}}$are the influence coefficients for the neighboring cells, and b is the contribution of the constant part of the source term (if any) and of the boundary conditions.

2.2. Simulated cases

A total of 214 cases were simulated in three different categories. In the first category, it was a mixture of air and tracer gas. Combinations of three different inlets and 10 different exhausts (six for ceiling inlet) were studied. Fig. 1 shows the room geometry with relative locations of inlets and exhausts. In addition, five different air flow rates—1,2,4,8 and 16 ACH (air changing per hour)—were analyzed resulting in a total of 130 cases studied. Results from this study were used to draw a conclusion as to the effect of inlet and exhaust position of the ventilation duct on the contaminant concentration. In addition to the above-mentioned cases, 78 cases were studied to determine the effect of

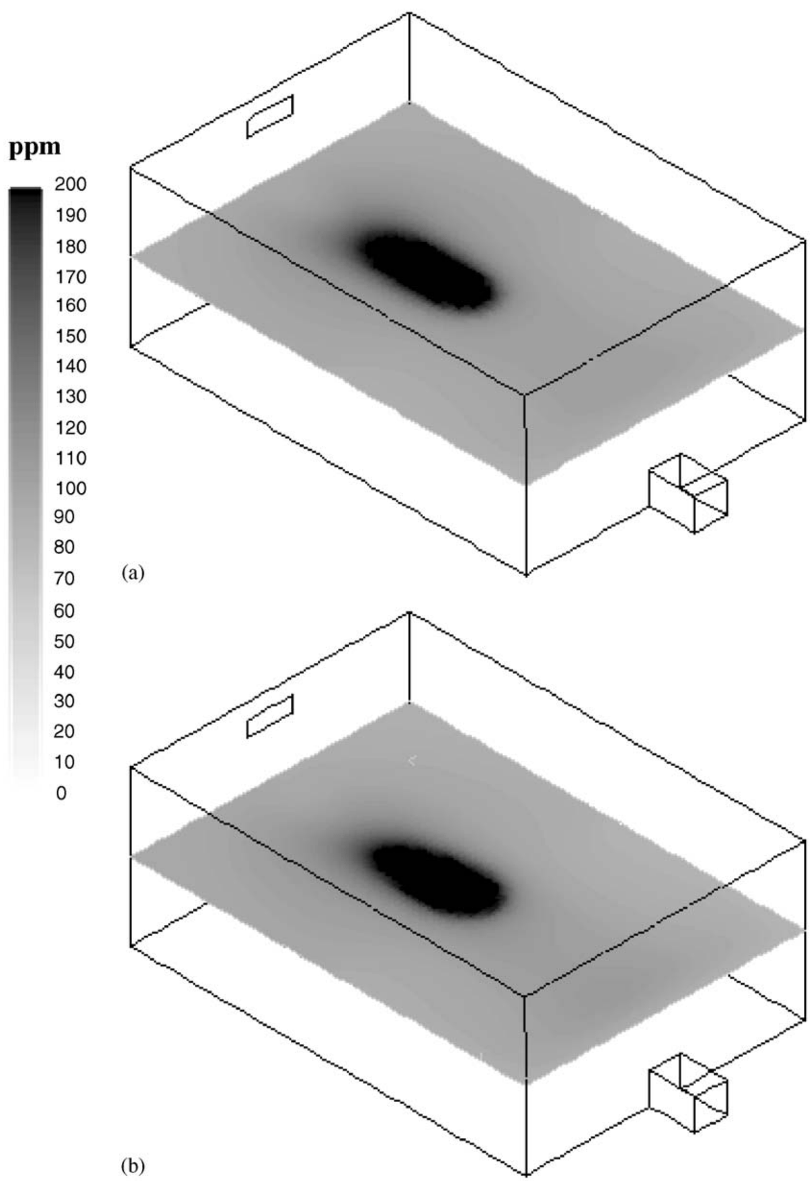

Fig. 2. Plots for grid independency showing contour of contaminant concentration on BZ for Inlet-1, and Exhaust-1, and 4.0 ACH flow. (a) domain with regular mesh, and (b) domain with finer mesh.

density difference between the contaminant and the room air. In the second category, the effect of density of the contaminant gas was observed by simulating three different air flow rates of 4, 8 and 16 ACH flow with similar inlets and exhausts combinations as in the first category. In the third category, it was studied if there was any change in the effect of inlet and exhaust position on concentration distribution due to ceiling inlet type. In this category, six different cases were numerically simulated with a flow rate of 4 ACH and with the mixture of air and tracer gas. Ceiling jet and ceiling diffuser (diffuses along longer sides of the room with a 15° angle from the ceiling) inlet types were analyzed.

3. Grid independency

To demonstrate the accuracy of the numerical results, in addition to validating the model, it is essential to demonstrate grid independence of the numerical result. For all CFD simulation cases the room domain was dicretized to 37284 cells of 0.15 m cube. Grid independence was established by changing the grid sizes and comparing the results. One selective case at 4 ACH for Inlet-1, Exhaust-1 for air and tracer gas (density equal to that of air) was simulated with a finer mesh of total 0.125 m cube 63 767 cells. The difference between the average room concentrations, average concentrations in the BZ and near-source BZs were found to be 0.1%, 0.85% and 1.55%, respectively. Fig. 2 shows the distribution of contaminant concentration on BZ plane for both regular and finer mesh.

4. Experimental set-up

To validate the computational results, experiments were performed in an existing rectangular chamber. Numerical results were compared with experimental results having identical boundary conditions. A room of $2.86\,\mathrm{m}(L) \times 2.86\,\mathrm{m}(W) \times 2.35\,\mathrm{m}(H)$ was constructed with an interior surface of plywood and insulated with Rmax-plus® on the exterior surface. A rectangular air inlet $0.39\,\mathrm{m} \times 0.24\,\mathrm{m}$ located at one upper corner, and a circular 0.1 m diameter exhaust located at the diagonally opposite corner of the inlet on the same wall of the room. A flow straightener was used at inlet section of the duct to create flow normal to the inlet opening. Flow velocities at inlet section was measured by a thermo-anemometer (Model 8350 VelociCalc™, TSI Incorporated, Saint Paul, MN) at 42 distributed points in the section from which an averaged uniform inlet air velocity was calculated.

A constant flow of tracer gas (99.5% propylene) was continuously emitted through a 0.1-m screened opening in the top of a 1-m high pedestal located at the center of the room. It was injected at the rate of $200\,\mathrm{cm}^3/\mathrm{min}$ which was bled from a compressed gas tank with a pressure regulator through a calibrated rotometer. Clean air, at the rate of 15 ACH was drawn into the room by a roof-mounted centrifugal exhaust fan, which discharges to the atmosphere. Air flow rate was achieved using an orifice plate restrictor and determined by measuring velocity along two perpendicular six-point traverses across the duct with the thermo-anemometer.

The tracer gas concentration was measured at 24 points in each of the three planes at different heights from the floor, bottom (0.4 m), middle (1.2 m) and top (2.0 m). For each sampling point a tygon tube (ID = 1/16″) of respective length was dropped from the ceiling. Concentration was also measured in the exhaust duct. The tubes were connected to a photoionization (PI) analyzer (PI101, HNu Instruments, MA) to read concentrations at one location at a time. PI analyzer was cleaned before each test and calibrated against a known concentration (100 ppm) of tracer gas in a Teflon bag. Sample gas stream was drawn through a manual valve system using a personal sampling pump. Concentration readings were recorded using a StowAway Voltage Logger (Onset Computer Corp. Onset, MA). The voltage logger was put off for 2-min after switching sampling points.

5. Results and discussion

5.1. Data validation

For the data validation, the numerical results obtained using the CFD were compared with the experimental results. Computations were performed with boundary conditions and room size as that of the experimental setup.

Fig. 3 shows a typical comparison between experimental and analytical results by line contour plot on the middle plane (1.2 m above the floor). Simulation results agreed with experimental results with respect to the shape of tracer gas distribution and the concentration levels. The average concentration of CFD results shows good agreement with experimental results for all three planes. The differences based on the experimental results were 3.88%, 2.13% and 2.22% for bottom, middle and top planes, respectively. Table 1 shows the data of all planes for both experimental and simulation results.

5.2. Effect of inlet and exhaust locations

From the numerical results, three different average concentrations of the contaminant were examined. They are: the average concentration of the RA, the average concentration in the BZ, 1.5 m above the floor, and

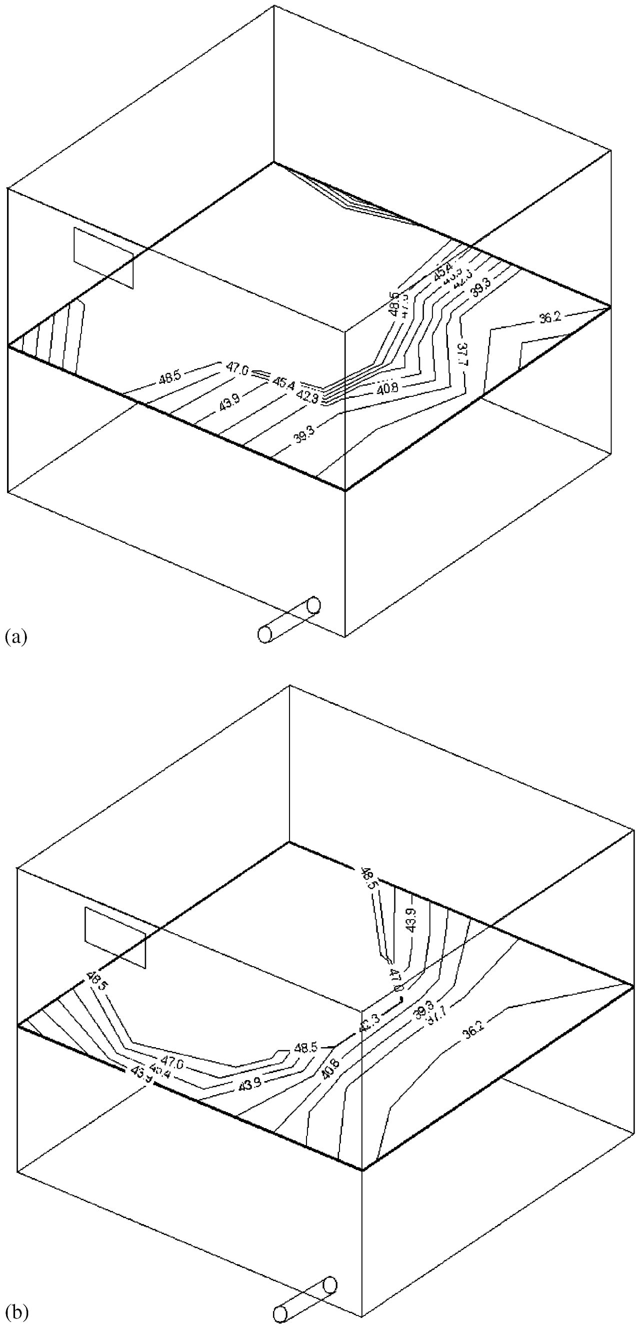

Fig. 3. Plots for data validation showing line contours of contaminant concentration on the plane 1.2 m above the floor. (a) Experimental results. (b) Simulation results.

average concentration of near-source BZ which is a 2.5 m square plane around the source on the BZ.

5.3. Inlet-1

Fig. 4 shows the average concentrations for Inlet-1 and different exhaust locations at a flow rate of 4.0 ACH. The average concentrations are shown for the RA, the BZ and the near-source BZ. Before discussing the concentrations, it is useful to study the particle tracks in the rooms. Fig. 5 shows the species path lines for Exhausts 9, 3 and 8 for Inlet-1 at flow rate 4.0 ACH. The path lines show the effect of exhaust locations on the flow which in turn determines how the contaminants are distributed in the room. Fig. 6 shows the concentration contours for the respective cases in the BZ with the range of 0–200 ppm.

As far as the room average is concerned, Exhausts 3, 4, and 5 located in the far corner side show the maximum average room concentration. A close examination of the path lines for 1–9 (Inlet-1 and Exhaust-9) shows that the recirculation of air is much longer which results in a better mixing of species. Also, the low pressure near the exhaust port plays an important role to suck the contaminant directly if the port is closer to the source. As Exhaust-9 is closer to the source than the others and also contaminant velocity is upward, this exhaust will help the outgoing air to entrain the contaminant better than any exhaust can do. For these reasons, Exhaust 9 results in the least concentration for Inlet-1 which is shown in Fig. 6. However, for Exhaust-3 it is clearly observed from the path lines that some fresh air is short-circuiting before it contributes in mixing. Comparing the flow pattern between that for Exhausts-3 and 8, it is observed that the amount of air which was short-circuiting through the Exhaust-3 is recirculating more for the case of Exhaust-8 which results in lower concentration for Exhaust-3 as shown in Fig. 6. Some of the findings for Inlet-1 are as follows.

In general, exhaust locations at the top of the wall (near the roof) are better than the exhausts near the floor, this is because inlet jet can pick up the upward moving contaminant and carry the contaminant out with it. Exhaust-2 is an exception, because it is directly opposite to the inlet jet in which case the inlet jet is short-circuited and allows fresh air to blow out of the room before mixing with the contaminant. This is evident from the species path lines. For Inlet-1 at 4.0 ACH flow rate average of average BZ concentration for all the exhausts located at the upper portion of the wall was found to be 141 ppm, whereas it was 158 ppm for the floor side exhausts.

Exhausts located on the same wall as the location of the inlet are always better than their respective exhausts on the far wall; for example, Exhaust-8 is better than Exhaust-3. This is because when the exhausts are in the opposite wall, the residence time for the ventilation air is small, and it gets less chance to be mixed with the contaminant to carry it out of the room. On the other hand, when the exhausts are on the same wall, air jet disperses, hits the opposite wall, disperses much more, and is thus recirculated and mixed well with the contaminant to push them out of the room. For Inlet-1 at 4.0 ACH flow rate average of average BZ concentration for all the inlet side exhausts was found

Table 1
Comparison of contaminant concentrations for both experimental and simulation results

Coordinates		Tracer Gas Concentration (ppm)					
		$Y = 2.0$ m		$Y = 1.2$ m		$Y = 0.4$ m	
X	Z	Exp.	Sim.	Exp.	Sim.	Exp.	Sim.
0.50	2.50	36.32	36.69	40.67	39.81	46.31	40.49
0.50	2.00	33.07	34.43	47.42	46.70	48.79	43.68
0.50	1.50	41.61	35.79	75.71	68.10	59.04	48.02
0.50	1.00	33.50	37.17	57.51	78.06	46.83	48.77
0.50	0.50	32.90	34.42	49.13	60.98	46.57	47.02
1.00	0.50	39.39	46.06	42.47	47.17	47.25	45.63
1.00	1.00	42.98	53.86	71.69	65.93	44.52	46.54
1.00	1.50	39.82	49.56	158.93	104.05	44.95	48.16
1.00	2.00	39.13	38.26	56.22	56.24	49.30	45.91
1.00	2.50	38.79	37.97	50.41	42.84	49.99	42.44
1.25	1.75	44.52	55.05	89.46	126.56	44.35	46.37
1.25	1.25	46.91	64.94	59.47	86.16	43.83	45.26
1.50	0.50	38.02	43.68	50.07	39.55	40.67	40.58
1.50	1.00	47.76	48.43	52.04	45.44	45.54	42.90
1.50	1.50	49.73	53.22	57.85	419.13	42.04	43.40
1.50	2.00	42.98	43.89	45.46	50.60	49.56	44.89
1.50	2.50	42.04	42.47	44.86	44.14	42.72	43.52
1.75	1.75	42.81	41.38	57.93	42.31	41.10	42.29
1.75	1.25	47.42	42.27	50.16	41.87	42.72	41.47
2.00	0.50	34.78	39.17	37.00	36.80	39.99	37.31
2.00	1.00	37.94	38.91	37.68	36.60	39.99	37.94
2.00	1.50	42.72	38.67	45.03	36.94	40.67	39.39
2.00	2.00	43.49	38.65	39.73	37.77	39.82	40.80
2.00	2.50	41.01	40.26	39.56	40.67	39.22	42.42
2.50	2.50	42.98	39.02	36.66	36.53	37.85	36.95
2.50	2.00	41.78	38.08	36.23	34.79	36.23	35.53
2.50	1.50	37.51	38.34	36.40	34.62	37.60	35.41
2.50	1.00	31.27	35.48	33.50	35.25	37.43	35.41
2.50	0.50	30.33	36.85	36.23	36.11	38.88	35.41
Average		40.12	39.23	52.95	51.82	43.58	41.89

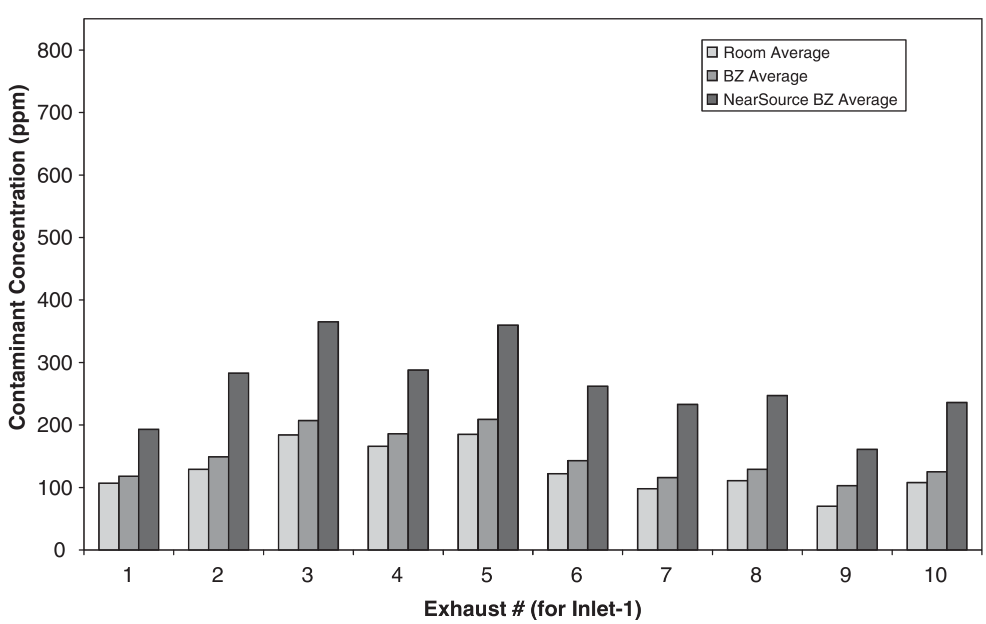

Fig. 4. Average contaminant concentration for Inlet-1 and 4.0 ACH flow rate.

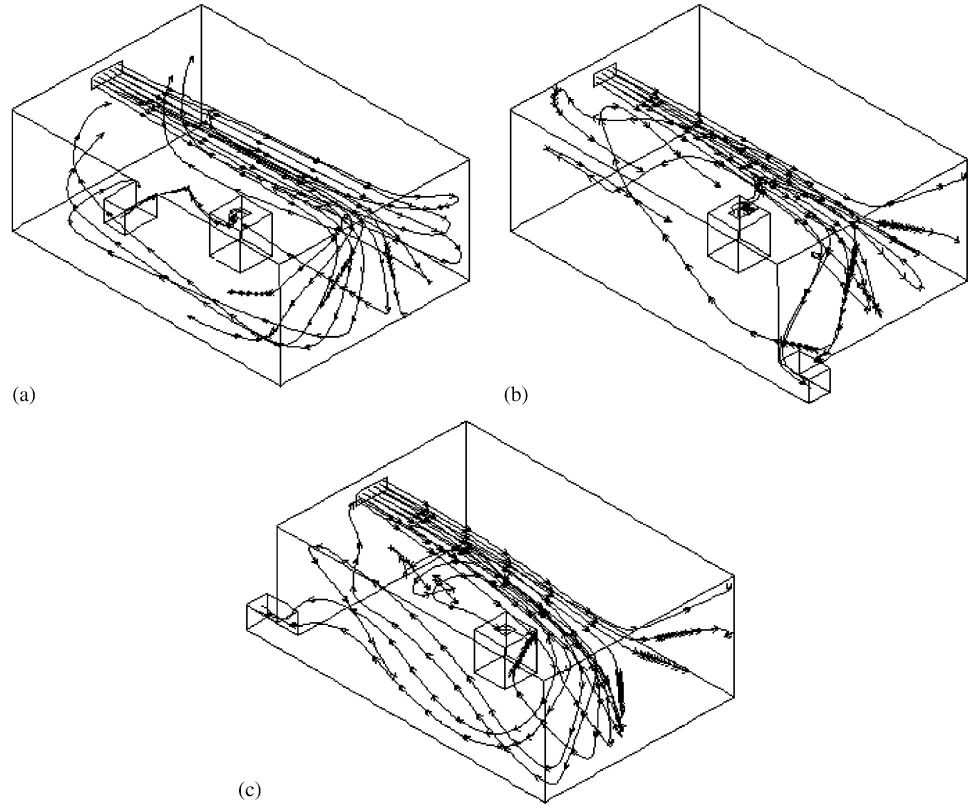

Fig. 5. Species path lines for Inlet-1 and 4.0 ACH flow. (a) Exhaust-9, (b) Exhaust-3, and (c) Exhaust-8.

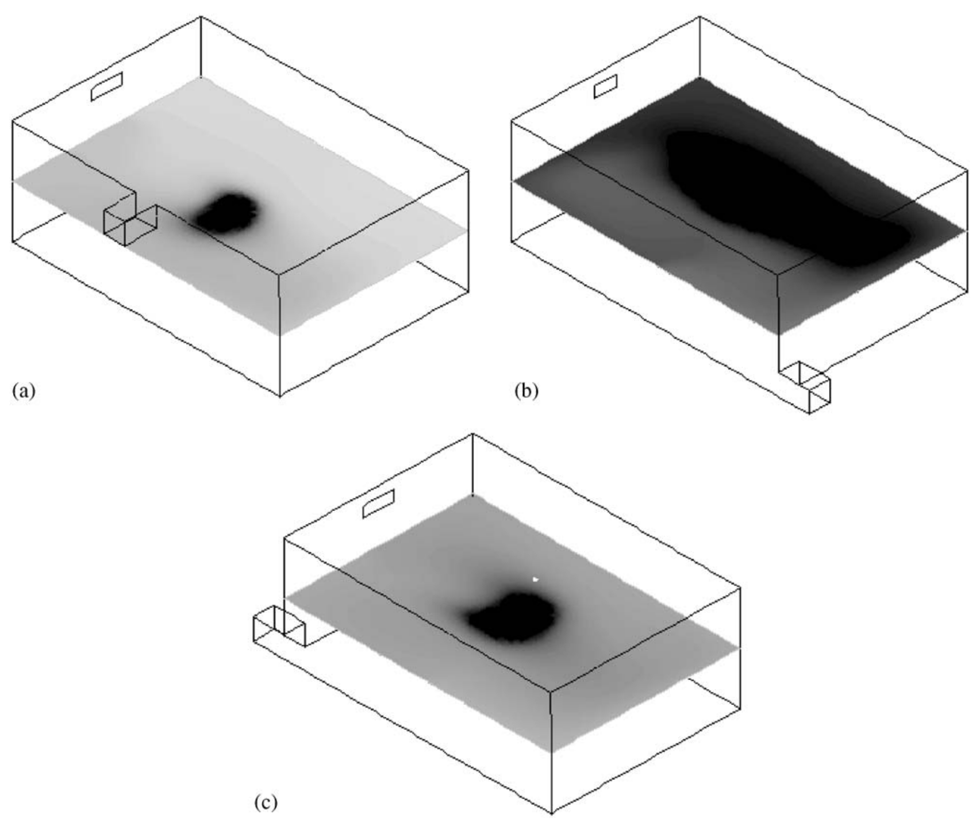

Fig. 6. Distribution of the contaminant concentration on BZ for Inlet-1 and 4.0 ACH flow. (a) Exhaust-9, (b) Exhaust-3 and (c) Exhaust-8. (contaminant concentration range from white-0 ppm to black-200 ppm).

to be 123 ppm, whereas it was 165 ppm for the opposite side exhausts.

Another finding is that the exhaust direction is not as important as its location in determining the concentrations in the room. Results of Exhausts 3 and 5 in Fig. 4 clearly show this.

5.4. Inlet-2

Fig. 7 shows the average concentrations for Inlet-2 and different exhaust locations at 4.0 ACH. For this inlet, findings are very similar to that for Inlet-1. Fig. 8 shows the species path lines, and the contaminant concentration distribution for Exhausts 1 and 2. For Exhaust-1, as observed from the figure, recirculation of air is much better while in case of Exhaust-2 most of the fresh air is being short-circuited. From the concentration fields the result is very obvious.

For Inlets-1 and 2, the room average concentration is lower than BZ average concentration which is again lower than near-source BZ concentration, although these averages do not show any difference in the findings discussed above.

5.5. Inlet-3, ceiling jet and ceiling diffuser

Fig. 9 shows the average concentrations for Inlet-3 and different exhaust locations at 4.0 ACH. From the figure it is evident that the exhaust location is not important for ceiling jet inlet type. Fig. 10 shows the path lines and concentration field for Inlet-3 and Exhaust-6 at 4.0 ACH flow rate. When the ceiling jet inlet is located directly above the source, the air entering into the room mixes and carries a significant amount of contaminant upward. This is the reason why the exhaust locations are not an important factor in determining the distribution of contaminant. Room average concentration is almost equal to the BZ concentration, because the contaminant is well mixed throughout the room. But the average concentration in the near-source zone is lower as the jet is directly injecting on it and taking away contaminants from the source. It is important to mention here that if the source is an evaporative source, ceiling jet directly above it will enhance the rate of source emission, and thereby it may increase the room contaminant concentration.

Ceiling diffuser cases are studied to compare the effect of diffuser and jet. The result shows that exhaust location is not an important factor for any of the ceiling inlets. Also, the type of ceiling inlet has almost no effect on room average concentration and BZ average concentration. But for ceiling diffuser, average concentration in the near-source BZ is much higher than that for ceiling jet. Species path lines show that jet directly falls upon the source which results in minimum near-source concentration while the diffuser causes the maximum concentration.

5.6. Effect of contaminant density

Flow rates of 4, 8, and 16 ACH are simulated to observe the effect of density on concentration of the contaminant for different inlet and exhaust combinations. The reason why the flow rates of 1 and 2 ACH were not simulated was that these flow rates were unstable and did not yield converged solutions. For

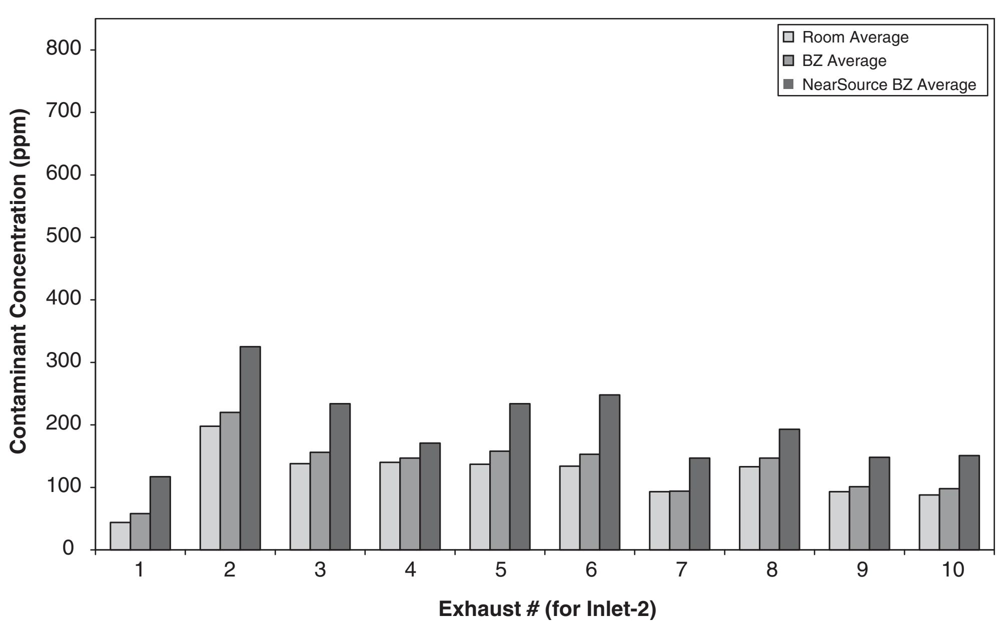

Fig. 7. Shows average contaminant concentration for Inlet-2 and 4.0 ACH flow rate.

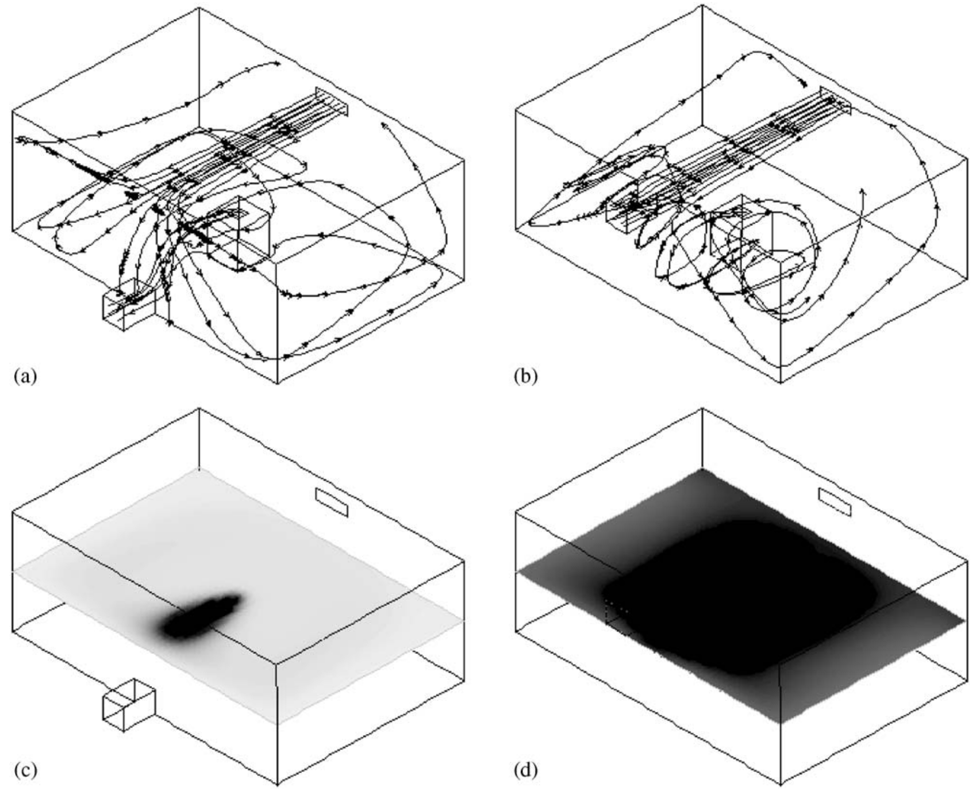

Fig. 8. Species path lines for Inlet-2 and 4.0 ACH flow with Exhaust-1 (a) and Exhaust-2 (b), and distribution of the contaminant concentration on BZ with Exhaust-1 (c) and Exhaust-2 (d) (contaminant concentration range from white-0 ppm to black-200 ppm).

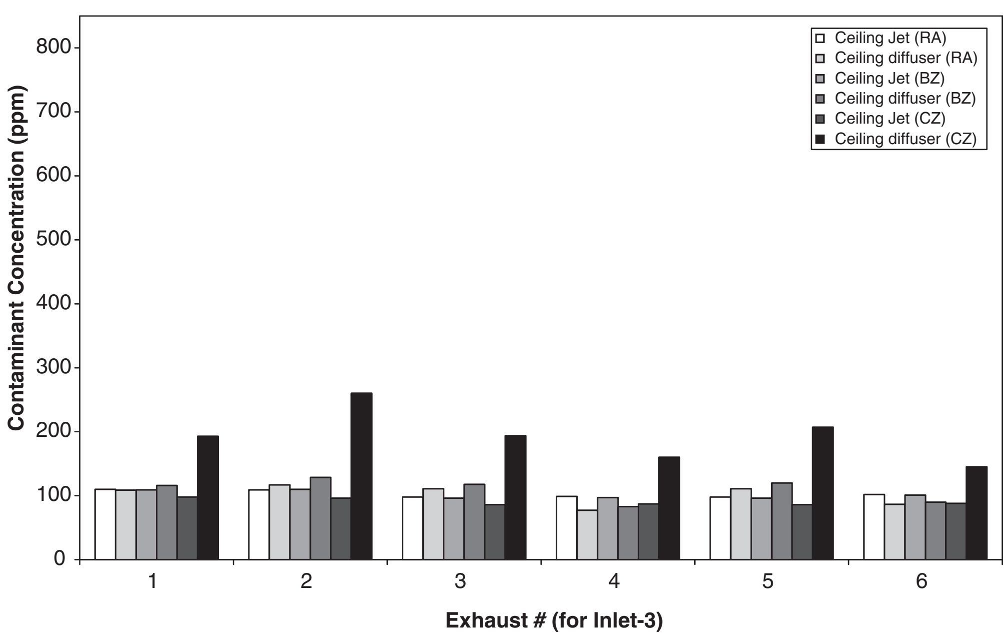

Fig. 9. Average contaminant concentration for ceiling jet and ceiling diffuser at 4.0 ACH flow rate.

lower flow rates, gravity effect (buoyancy) of the dense contaminant is predominant over the convective effect, so after some iterations the solution becomes unstable.

Figs. 11 and 12 show the average contaminant concentration for dense and light source of Inlets-1 and 3. Based on the simulated flow rates, it is obvious that when flow rate is higher, density of the contaminant

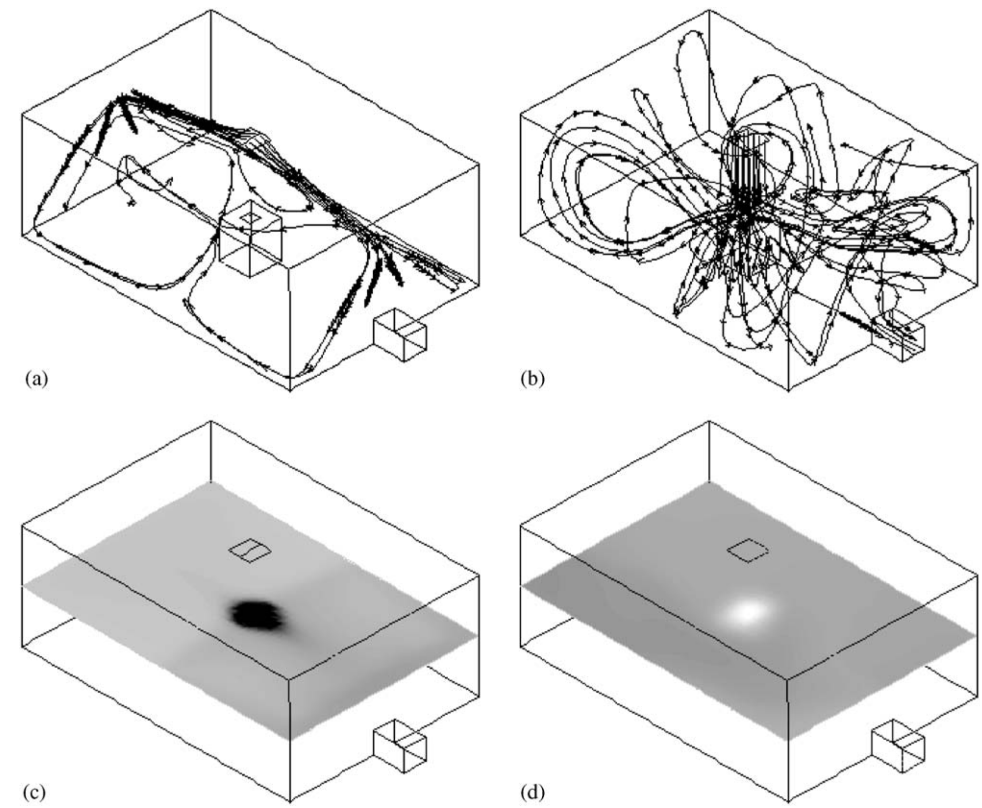

Fig. 10. Species path lines for Inlet-3, Exhaust-6, and 4.0 ACH flow with diffuser type (a) and jet type (b), and distribution of the contaminant concentration on BZ with diffuser type (c) and jet type (d) (contaminant concentration range from white-0 ppm to black-200 ppm).

has almost no effect on concentration distribution, because at higher flow rates the inertial effect of the fluid result in predominant forced convective transport.

For 4 ACH flow, some effect of density on concentration was found. The respective results for room concentration was 128 ppm with tracer gas and 135.5 ppm for the denser gas, and for BZ concentration 148.5 ppm with tracer gas and 134.9 ppm with the dense gas. Of course it is expected that with lower flow rates the effect will be more pronounced.

Choice of exhaust locations between near roof and near floor is affected by the density of contaminant gas. For heavier gas and lower flow rate, near-floor exhaust locations are relatively a better choice than near-roof locations. The average of BZ concentration for Inlet-1 at 4.0 ACH was found to be 132.83 for near-floor exhausts while 138 ppm was found for near-roof exhausts.

5.7. Effect of air flow rate

This effect can be studied by referring to Fig. 11. Simulated cases with tracer gas source shows that the concentration of contaminant is nearly inversely proportional to ACH, and it has no effect on the judgment of finding the best inlet and exhaust locations. This is intuitive that as the volume flow rate of the clean air is larger, it will mix and dilute the concentration of the contaminant. For dense gas, concentration is not exactly inversely proportional at lower flow rates. At lower flow rates, the buoyancy may have a greater effect than the forced convection. But at higher rates, buoyancy is no more important, and the results are similar to that for tracer gas. As was mentioned before, for dense gas flow rates also affect the choice of exhaust locations.

5.8. Effect of thermal gradient

The focus of this paper was to study the effect of various inlet and outlet locations and also to study the effect of the relative density of the source gas during isothermal conditions. A detailed experimental and computational investigation was indeed performed by this research group for non-isothermal conditions. The result of the finding is presented by Lee [15] in her Ph.D. dissertation. It was found in the study that the concentration distribution for simulated winter and summer conditions were greatly different in the breathing zone. For detailed results, please refer to Lee [15].

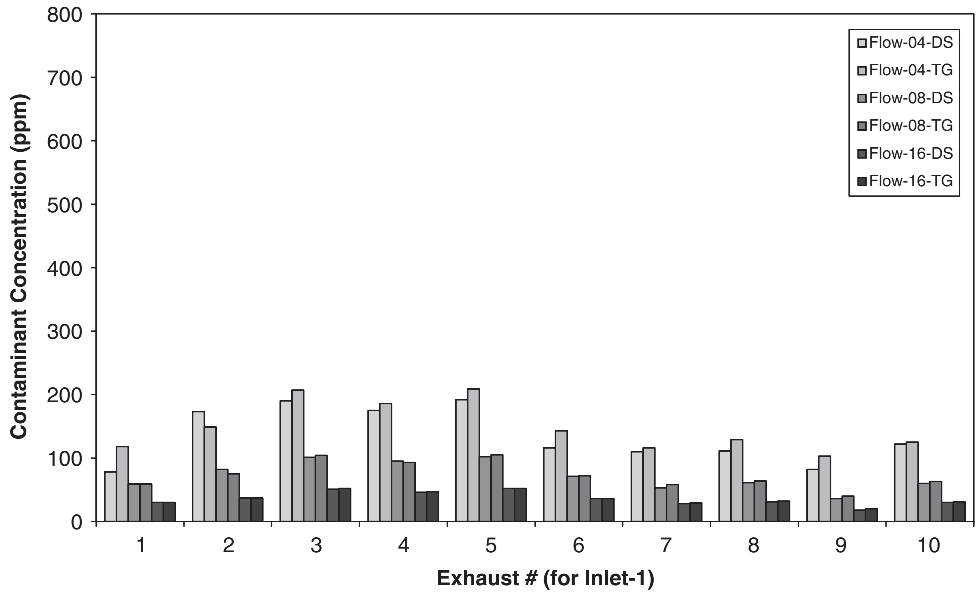

Fig. 11. Average contaminant concentration for dense and light source in the breathing zone (Inlet-1).

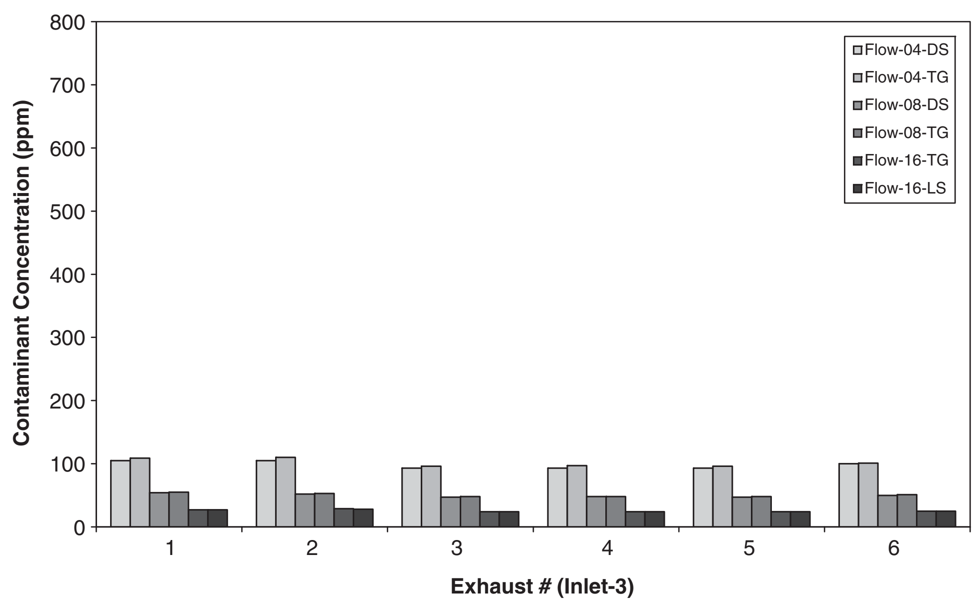

Fig. 12. Average contaminant concentration for dense and light source in the breathing zone (Inlet-3).

6. Conclusions

A detailed computational investigation was performed to study physical factors that affect distribution of contaminant concentration in a workroom. The computational study was validated with experimental finding. The following conclusions are obtained from this study.

For the Inlet-location of the make-up fresh air on the side wall, it was determined that the exhausts near the roof were better than exhausts near the floor (for example, Exhaust-10 is better than Exhaust-8 for Inlet-1) except for Exhaust-2, which was due to short circuiting of fresh inlet air.

Exhausts located on the same side as the inlet-location wall were generally better than that of the opposite side wall (for example, Exhaust-10 is better than Exhaust-4 for Inlet-1).

For ceiling inlets, location of the exhausts was not important. Also, type of ceiling inlet (jet or diffuser) had very little effect on average concentration except at near-source zone

At lower dilution air flow rates (4 ACH or less), density of the gaseous contaminant had a significant effect on the concentration distribution in the room because buoyant flow was significant. For heavier gas source, exhaust locations near the floor was a better choice than near the roof. For ceiling inlet, gas density had very little effect on concentration. At higher dilution flow-rates the inertial effects dominated as a result of the contaminant density had negligible effect on concentration.

It was also observed that for all exhaust locations, contaminant concentration was inversely proportional to air inlet flow rate when air and contaminant gas had comparable densities. This was not true when the source gas was heavier than the room air; in that case, it depended on the location of the exhausts.

Ceiling inlet resulted in uniform concentration distribution in the room. The type of ceiling inlet-diffuser or jet had negligible effect on the room average and breathing zone concentration.

References

[1] Lidwell OL, Lovelock JE. Some methods for measuring ventilation. Journal of Hygiene (Cambridge) 1946;44:326–32.

[2] Brief RS. Simple way to determine air contaminants. Air Engineering 1960;2:39–40.

[3] Jayjock MA. Assessment of inhalation exposure potential from vapors in the workplace. American Industrial Hygiene Association Journal 1988;49:380–5.

[4] Fiegley CE, Bennett JS, Lee E, Khan JA. Improving the use of mixing factors for dilution ventilation design. Applied Occupational and Environmental Hygiene 2002;17(5):333–43.

[5] Furtaw EJ, Pandian MD, Nelson DR, Behar JV. Modeling indoor air concentrations near emission sources in imperfectly mixed rooms. Air and Waste Management Association 1996;46: 861–8.

[6] Hemeon WCL. Plant and process ventilation. 2nd ed. NY: Industrial Press Inc; 1963.

[7] Heinsohn RJ. Industrial ventilation engineering principles. NY: Wiley; 1991.

[8] Nicas M. Estimating exposure intensity in an imperfectly mixed room. American Industrial Hygiene Association Journal 1996; 57:542–50.

[9] Bennett JS, Fiegley CE, Khan JA, Hosni MH. Comparison of mathematical models for exposure assessment with Computational Fluid Dynamic Simulation. Applied Occupational and Environmental Hygiene 2000;15(1):131–44.

[10] Sherman MH. Tarcer gas techniques for measuring ventilation in a single zone. Building and Environment 1990;25(4):365–74.

[11] Waters JR, Simons MW. The evaluation of contaminant concentrations and air flows in a multizone model of a building. Building And Environment 1987;22(4):305–15.

[12] Fiegley CE, Bennett JS, Khan JA, Lee E. Performance of deterministic workplace exposure assessment models for various contaminant source, air inlet, and exhaust locations. American Industrial Hygiene Association Journal 2002;63:402–12.

[13] Nicas M, Jayjock M. Uncertainty in exposure estimates made by modeling versus monitoring. American Industrial Hygiene Association Journal 2002;63(3):275–83.

[14] Lee E, Fiegley CE, Khan JA. An investigation of air-inlet velocity in simulating the dispersion of indoor contaminants via Computational Fluid Dynamics. Annals of Occupational Hygiene 2002; 46(8):701–12.

[15] Lee E., 2004. An investigation of physical factors for estimating exposure to airborne contaminants. PhD dissertation, Department of Environmental Heath Sciences, University of South Carolina, Columbia, SC 29208.